



FRONTIERS IN ELECTRONICS AND COMMUNICATION ENGINEERING

ISSN: (3065- 4106)



editor.fece@gmail.com



<https://multisciajournals.com/journals/index.php/fece>

Evaluation of ESPRIT DOA Estimation Algorithm, Root-MUSIC, and MUSIC Performance

Rezarta Islamaj Dogan
Department of ECE

Article Info

Received: 25-06-2025 Revised: 20-07-2025 Accepted: 08-08-2025 Published: 18-08-2025

Abstract— Determining a mathematical function known as a pseudospectrum that indicates the angle at which a signal is impinging on the antenna array is known as "direction of arrival estimation." By concentrating reception and transmission solely in the estimated direction, this estimation increases fidelity and provides a means of suppressing interferers, making it an effective way to enhance the quality of service in a communication system. The effectiveness of the method used for the estimation has a significant impact on this improvement. There are numerous DOA algorithms, including ESPRIT, MUSIC, and Root-MUSIC. This study examines how well these three algorithms perform in terms of complexity, accuracy as measured and described by the CRLB, and memory needs across a range of array sizes and settings. The three high-resolution techniques are shown to be reliant on the array size and operation conditions.

Keywords— Arrival direction, autocorrelation matrix, eigenvalue decomposition, music, ESPRIT, and CRLB

I. INTRODUCTION

One of the areas of engineering that is expanding the fastest is wireless communication. The advancements in communication equipment research and design have made this necessary [1], [2]. Cellular connectivity was the first, followed by the internet to the point where these services are available at any time and from any location. However, when the distance between the sending and receiving nodes increases, the Quality of rvice (QoS) degrades. By intensifying and concentrating the transmission solely in the direction of the receiver and vice versa for the receiver, estimating the direction of a transceiver is a useful technique for enhancing the quality of service (QoS) between a node and a transceiver [3]–[5]. Antenna arrays having the additional ability to predict the Direction of Arrival (DOA) of all incoming signals are used to do this. The performance of the used algorithm plays a major role in the aforementioned improvement. The size of the array, the amount of impinging signals, the distance between elements, and the number of snapshots utilized in the estimate phase all affect how well a DOA method performs. There are numerous DOA methods, such as those based on eigenvalue decomposition and quadratic types like CAPON. MUSIC

II. Waweru works at Dedan Kimathi University of Technology's Electrical & Electronic Engineering Department, P.O. Box 657-10100, Nyeri (corresponding author, phone: +254724876363; email: waweru@ymail.com). Konditi works at MultiMedia University College of Kenya's Department of Electrical and Communication Engineering, P.O. Box 30305-00100, Nairobi. Langat works at Jomo Kenyatta University of Agriculture and Technology's Telecommunication & Information Engineering Department, located at P.O. Box 62000-00200, Nairobi. ESPRIT and variations on it. Algorithms based on eigenvalue decomposition manipulate the signal autocorrelation matrix to produce signal and noise subspaces, from which the angles of arrival of impinging signals are retrieved. In order to determine the best technique and design for a particular setting, this research aims to evaluate the performance of three DOA algorithms based on the number of array elements and the Signal to Noise Ratio (SNR). MATLAB software was used to build and simulate the MUSIC, Root-MUSIC, and

ESPRIT algorithms for signals operating at 2.4GHz for a ULA with inter-element spacing of λ . The Cramer-Rao Lower Bound (CRLB) for DOA estimation is obtained in Section II of this study after the signal model of a N element uniform linear array receiving M signals from directions $\theta_1, \theta_2, \dots, \theta_M$ is derived.

III. III. The mathematical foundations of the three methods are briefly explained in Sections IV–VI. Section VII presents the simulation findings, while Sections VIII and IX provide the discussion and conclusion, respectively.

IV. SIGNAL MODEL

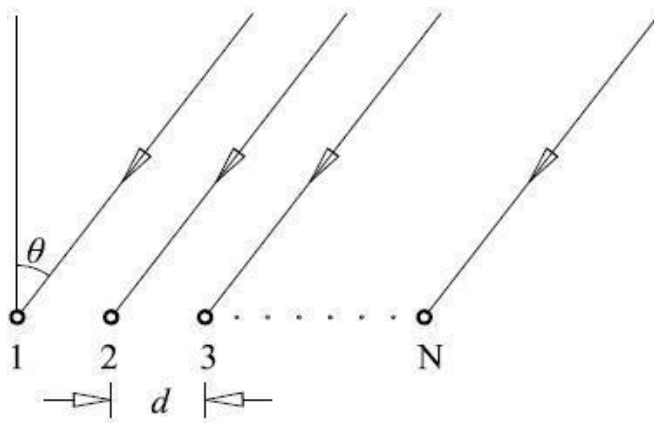


Fig. 1. Uniform linear array.

As illustrated in Fig. 1, consider a uniform linear array (ULA) with N identical elements spaced apart by d. At an angle θ to the array axis, a far field signal is impinging on this array. The line path from the source to the i th element, using element 1 as the reference, is shorter than

that to the 1st element. If the received signal at sensor 1 is $x_1(t) = s(t)$, it is delayed at sensor i by

$(i - 1)d \sin \theta$ two: array steering vector and the noise subspace, therefore is a null for a particular Angle of Arrival (AOA):

For a uniform linear array with N elements and M signals $s_1(t), s_2(t), \dots, s_M(t)$ arriving from directions $\vartheta_1, \vartheta_2, \dots, \vartheta_M$, and in the presence of noise $\mathbf{n}(t)$, the received signal $\mathbf{x}(t)$ is Then the received signal at sensor i is

$$\begin{aligned} x_i(t) &= e^{-j\omega\tau_i} x_1(t) = e^{-jkd(i-1)\sin\theta} s(t) \text{ given by} \\ \mathbf{x}(t) &= \mathbf{A}s(t) + \mathbf{n}(t) \end{aligned} \tag{7}$$

(2) Putting received signals from all N elements together. Defining an

$N \times N$ autocorrelation matrix of the received signal

\mathbf{R}_{xx} as

$$\mathbf{R}_{xx} = E\{\mathbf{x}(t)\mathbf{x}^H(t)\} = \mathbf{A}\mathbf{R}_{ss}\mathbf{A}^H + \sigma^2\mathbf{I} \tag{8}$$

$$\mathbf{R}_{ss} = E\{s(t)s^H(t)\} = \text{diag}\{\sigma_1^2, \dots, \sigma_M^2\} \tag{9}$$

eigenvectors making a subspace $E=[e_1, e_2, \dots, e_N$

\mathbf{R}_{xx} has N eigenvalues $[\lambda_1, \lambda_2, \dots, \lambda_N]$ and N associated
]. Sorting

where $\mathbf{a}(\vartheta)$ is called the steering vector.

If there are M signal sources, received by the array arriving at angles $\vartheta_1, \vartheta_2, \dots, \vartheta_M$, we get a signal model

$$\mathbf{x}(t) = \mathbf{A}s(t) \quad (4)$$

where the vector \mathbf{A} is the array steering vector having the following vandermode structure.

$$\mathbf{A} = \begin{bmatrix} 1 & 1 & \dots & 1 \\ e^{-j2\psi_1} & e^{-j2\psi_2} & \dots & e^{-j2\psi_M} \\ \vdots & \vdots & \ddots & \vdots \end{bmatrix} \quad (5)$$

the N eigenvalues from the smallest to the largest, the subspace E can be decomposed into two subspaces:

$$E = [e_1, \dots, e_M, e_{M+1}, \dots, e_N] \quad (10)$$

$$E_N = [E_N \ E_S] \quad (11)$$

E_N is the $N \times (N - M)$ noise subspace composed of the eigenvectors associated with the noise, whereas E_S is the $N \times M$ signal subspace composed of the eigenvectors

$$e^{-j(N-1)\psi_1} \quad e^{-j(N-1)\psi_2} \quad \dots \quad e^{-j(N-1)\psi_M}$$

associated with the arriving signal. Due to the orthogonality of the noise subspace and the array steering vector at the angles of arrival $\vartheta_1, \vartheta_2, \dots, \vartheta_M$, the

V. CRAMER-RAO LOWER BOUND

Cramer-Rao Lower Bound provides an algorithm independent means of assessing and comparing the accuracy matrix product $\mathbf{a}^H(\vartheta)E_N E^H \mathbf{a}(\vartheta)$ is zero for this angles. The reciprocal of this matrix product creates sharp peaks at the angle of arrival. Thus the MUSIC pseudospectrum is given and performance of a DOA algorithm. The CRLB on the variance of direction estimation errors provides a useful characterization of the achievable accuracy

$$DOA P(\vartheta) = \frac{1}{|\mathbf{a}^H(\vartheta)E_N E^H \mathbf{a}(\vartheta)|} \quad (12)$$

system. This is achieved by comparing the Mean Square Error(MSE) with the CRLB [6], [7].

The CRLB theorem states that for a length N vector of received signal \mathbf{x} dependent on a set of parameters P, and corrupted by additive noise, the variance of an unbiased estimate of the p^{th} estimate is greater than the cramer-rao lower bound.

The CRLB of a DOA estimation problem is given by V. ROOT-MUSIC

This is a variant of MUSIC algorithm that employs more information than MUSIC [10]. Unlike MUSIC which involves plotting the pseudospectrum against the angles and searching for the peaks, ROOT-MUSIC involves finding the roots of a polynomial.

Starting with the pseudospectrum of MUSIC algorithm

$$P(\vartheta) = \frac{1}{r[N(N^2 - 1)(kd)^2 \sin^2 \vartheta]} \quad \text{ar}(\vartheta) \geq \text{CRLB} \quad (13)$$

VI. MUSIC

Multiple Signal Classification (MUSIC) is a popular high resolution algorithm based on eigenstructure technique. The main idea behind this DOA algorithm is that of performing $\mathbf{a}^H(\vartheta)E_N E^H \mathbf{a}(\vartheta)$ defining $C = E_N E^H$, the denominator of equation 12 above can be rewritten as

14) eigenvalue decomposition on the correlation matrix [8], [9], separating it into two subspaces: signal subspace

and the noise subspace. Since the signal subspace is spanned by the array steering vector of the received signals, this makes the steering vector orthogonal to the noise subspace. The product of the m^{th} element $a_m(\vartheta)$ of the array steering vector is defined as

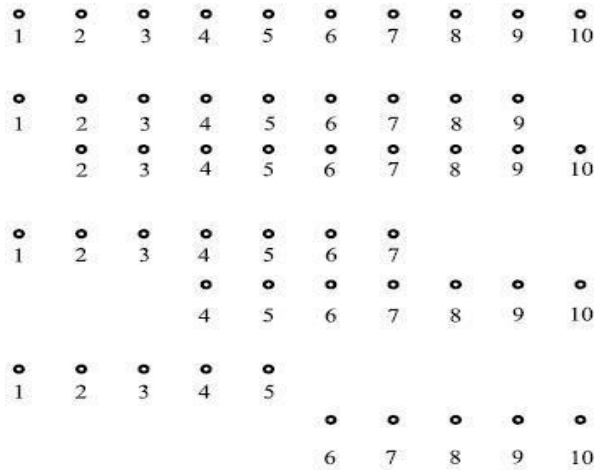
$$a_m(\vartheta) = e^{-jkd m \sin \vartheta}, \quad m = 0, 1, \dots, N - 1 \quad (15)$$

The denominator, thus can be rewritten as

$$a^H(\vartheta)Ca(\vartheta) = \sum_{m=0}^{N-1} \sum_{n=0}^{N-1} e^{-jkd m \sin \vartheta} C_{mn} e^{jkd n \sin \vartheta}$$

(16)

$A = -N + 1$



$$C_A e^{jkd A \sin \vartheta}$$

where C_A is the sum of the elements along the A^{th} diagonal of C .

Letting $z = e^{-jkd \sin \vartheta}$, equation 16 above simplifies to

$$D(z) = \sum_{A=-N+1}^{-1} C_A z^A \quad (17)$$

The roots of $D(z)$ that lie closest to the unit circle correspond to the poles of the MUSIC pseudospectrum. These $2(N - 1)$ roots can be written as

$$z_i = |z_i| e^{j \arg(z_i)}, \quad i = 1, 2, \dots, 2(N - 1) \quad (18)$$

Choosing those roots inside the unit circle whose magnitude $|z_i| < 1$, and comparing $e^{j \arg(z_i)}$ to $e^{-jkd \sin \vartheta}$ gives

Fig. 2. ULA decomposition in ESPRIT algorithm.

From equation 20, correlation matrices \mathbf{R}_{11} and \mathbf{R}_{22} of the signals in the two subarrays can be estimated as

$$\vartheta = -\sin^{-1} \frac{\arg z_i}{kd} \quad (19)$$

$$\mathbf{R}_{11} = E\{x_1(t)x_1^H(t)\} \quad (20)$$

$$\mathbf{R}_{22} = E\{x_2(t)x_2^H(t)\} \quad (23)$$

1
2

Estimation of Signal Parameters via Rotational Invariance Technique (ESPRIT) algorithm involves

subarrays, corrupted by additive white gaussian noise $n_1(t)$ and $n_2(t)$ respectively. From M eigenvalues of Φ , angles of arrival can be estimated

$$\vartheta = \sin^{-1} \frac{\arg(\lambda_i)}{k\Delta} \quad (27)$$

$$x_2(t) = \mathbf{A}\Phi s(t) + n_2(t) \quad (20)$$

where $x_1(t)$, $x_2(t)$, $n_1(t)$ and $n_2(t)$ are $M \times 1$ matrices. \mathbf{A} is the $S \times M$ steering matrix and the variable Φ is $M \times M$ diagonal matrix called the rotation operator.

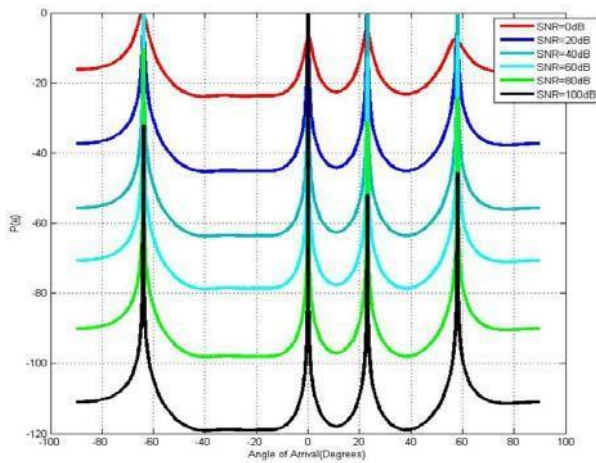
$$\Phi = \text{diag}\{e^{j\psi_1}, e^{j\psi_2}, \dots, e^{j\psi_M}\} \quad (21)$$

where

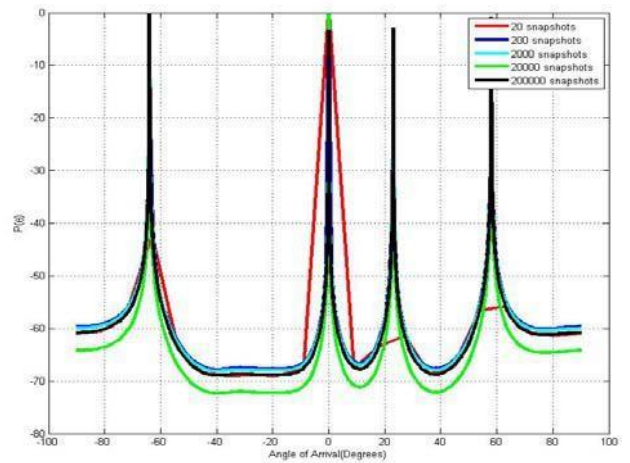
$$\psi_i = -2k\Delta \sin \vartheta_i; \quad 1 \leq i \leq M \quad (22)$$

VI. SIMULATION RESULTS

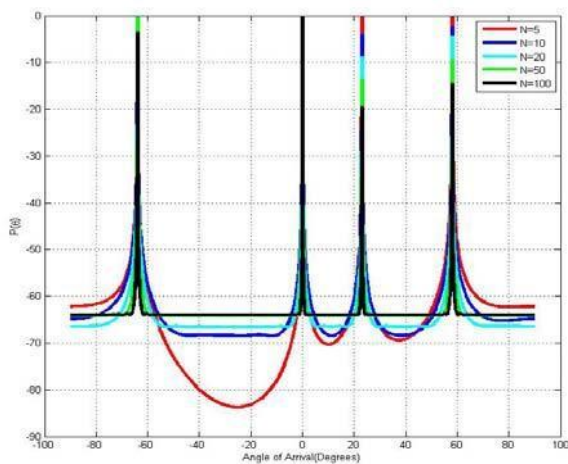
Simulations were done in MATLAB software for angles of arrival $\vartheta_1 = -64^\circ$, $\vartheta_2 = 0^\circ$, $\vartheta_3 = 23^\circ$ and $\vartheta_4 = 58^\circ$ respectively. The array size was held to 8 elements as the values of SNR were varied from 0-100dB in steps of 20dB. This was repeated holding SNR to 50dB and varying the array size from 5-100 elements.



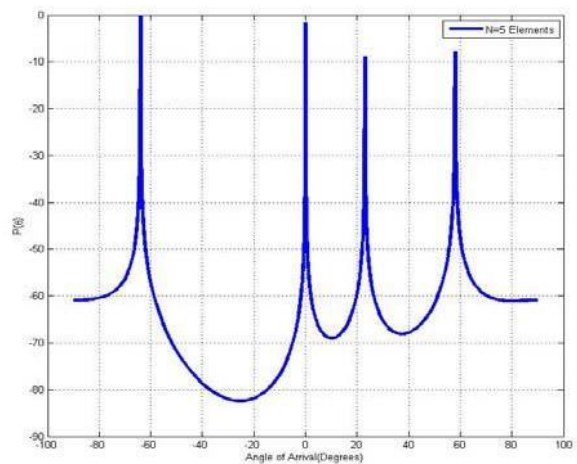
(a) MUSIC for varying SNR



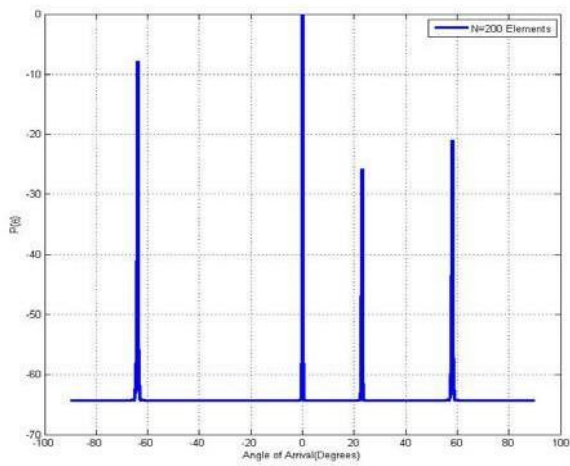
(b) MUSIC for varying snapshots



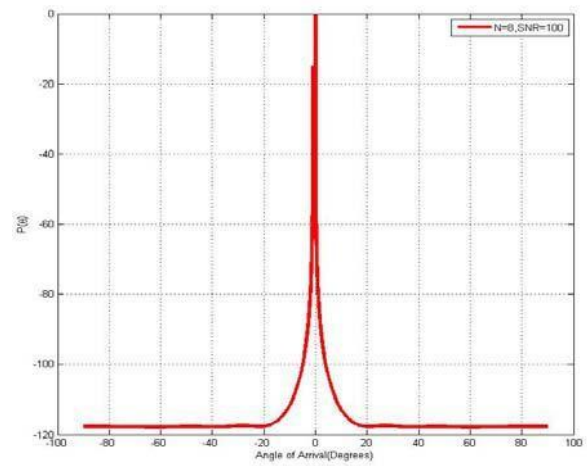
(c) MUSIC for varying array size



(d) MUSIC for a 5 element array



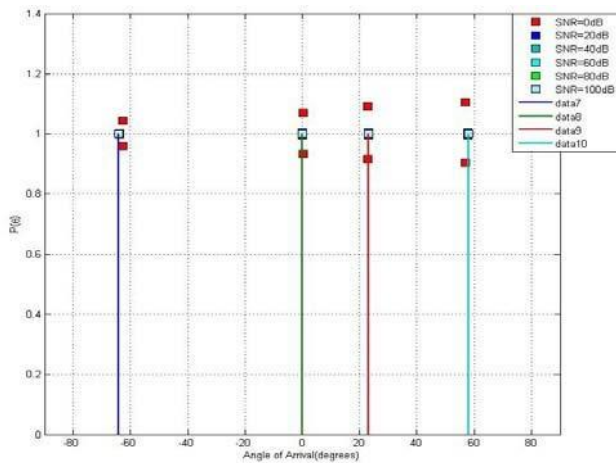
(e) MUSIC for a 200 element array



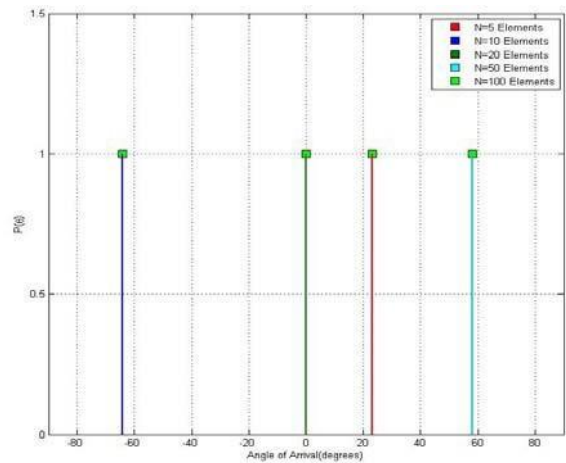
(f) MUSIC for two angles closely spaced

Fig. 3. Performance of MUSIC algorithm

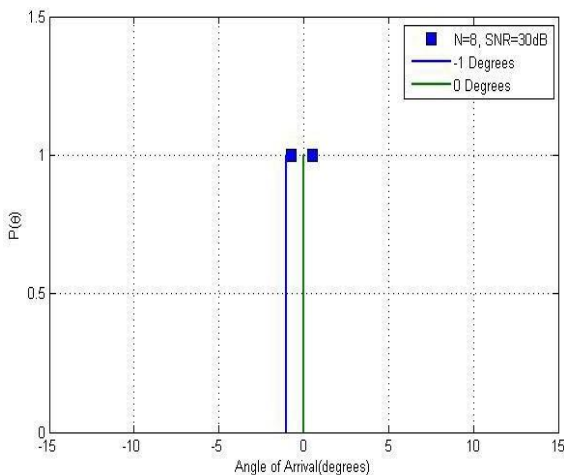
Fig. 3 shows the performance of MUSIC algorithm in various operating conditions. Fig. 3a shows the performance of this algorithms in an environment with varying SNR. For low values of SNR, 0dB, the spikes depicting the arrival of a



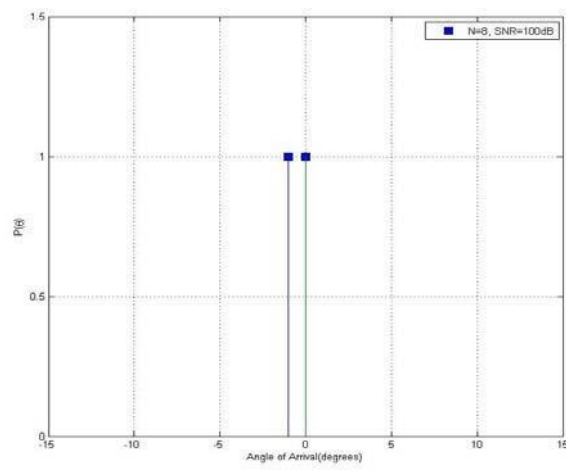
(a) Root-MUSIC for varying SNR



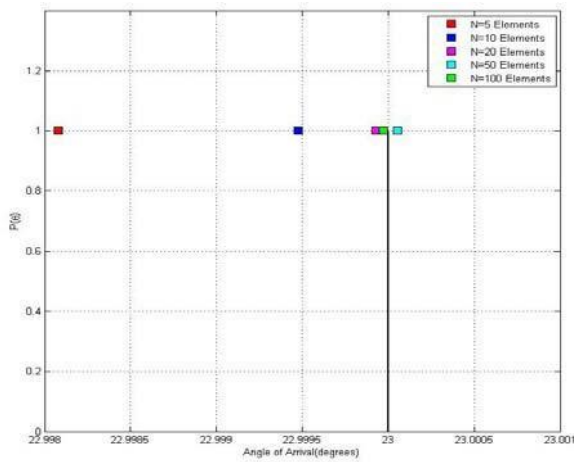
(b) Root-MUSIC for varying array size



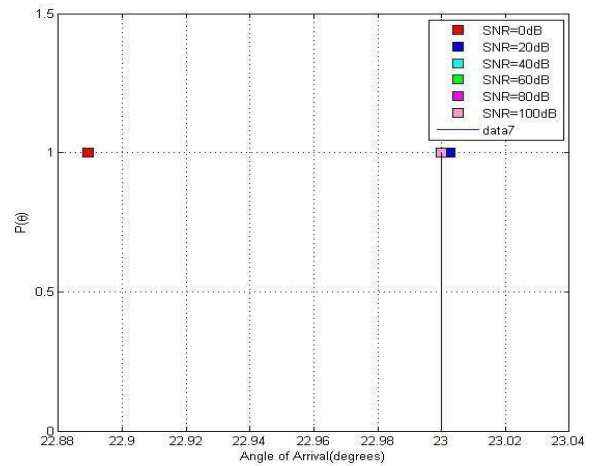
(c) Root-MUSIC for two closely spaced angles-30dB



(d) Root-MUSIC for two closely spaced angles-1000B



(e) Root-MUSIC at 23° for varying array size

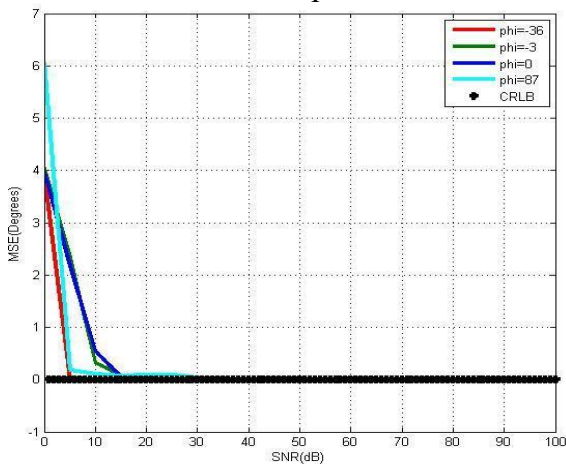


(f) Root-MUSIC at 23° for varying SNR

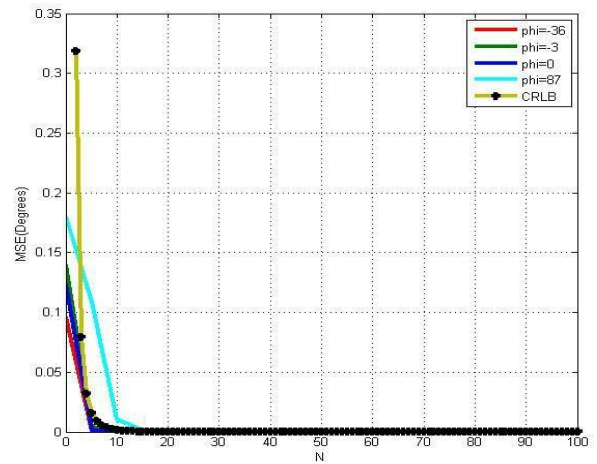
Fig. 4. Performance of Root-MUSIC

signal from certain direction are small and the response is almost flat. It is thus difficult to exactly extract the angles of arrival. As the values of SNR increase, however, the resolution of the algorithm is observed to improve

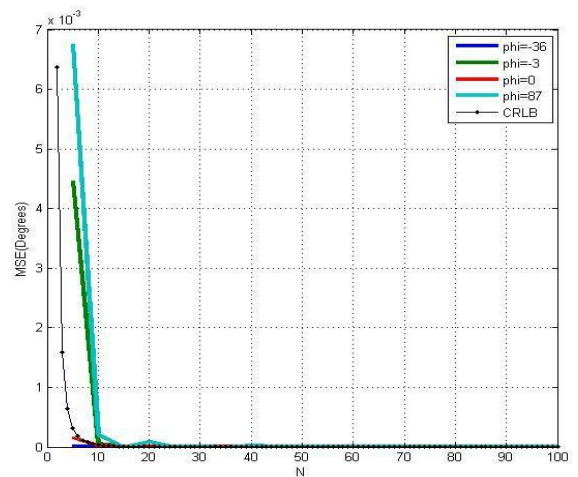
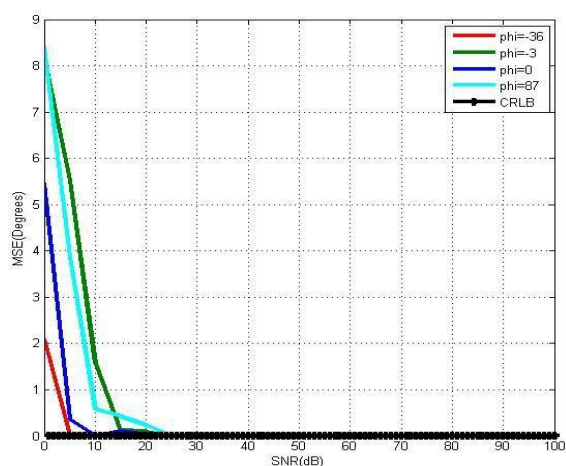
considerably and the spikes become more definite. This is attributed to the fact that for low SNR the difference between the eigenvalues associated with the signal and those associated with the noise become smaller and the peaks



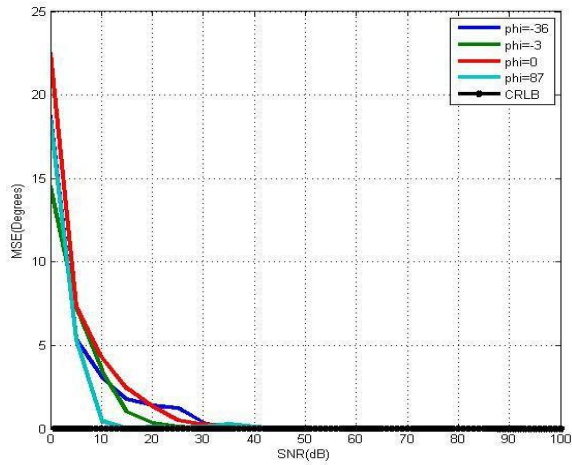
(a) MSE of MUSIC for varying SNR



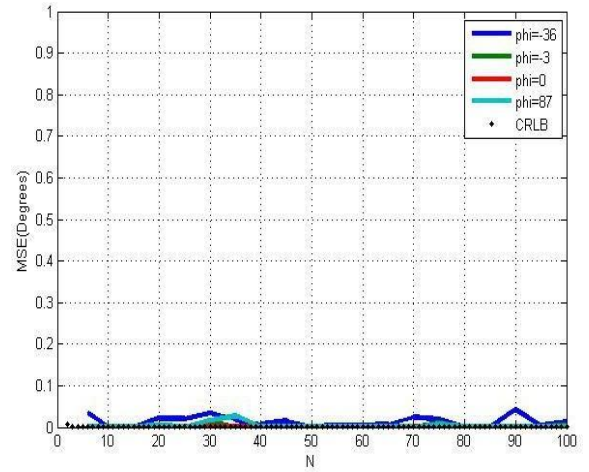
(b) MSE of MUSIC for varying array size



(c) MSE of Root-MUSIC for varying SNR



(d) MSE of Root-MUSIC for varying array size



(e) MSE of ESPRIT for
varying S

NR

(f) MSE of ESPRIT for varying array size

5. MSE in various environments

TABLE I
 ACCURACY OF ESPRIT FOR VARYING SNR

SNR	-64°	0°	23°	58°
0dB	-62.8826	1.3855	35.1460	57.0785
10dB	-65.4913	-0.0669	28.2430	57.5258
20dB	-64.3173	0.1507	24.2929	58.9783
30dB	-64.0421	0.0655	23.2738	58.3887
40dB	-64.0120	-0.0120	22.8796	58.0220
50dB	-64.0092	0.0001	23.0749	57.9863
60dB	-63.9981	0.0026	23.0057	57.9986
70dB	-64.0011	0.0004	22.9964	58.0001
80dB	-63.9997	0.0004	22.9997	58.0010
90dB	-63.9999	0	22.9994	58.0000
100dB	-64.0000	0	22.9997	57.9999

TABLE II

ACCURACY OF ESPRIT FOR VARYING ARRAY SIZE $\vartheta_1=1^\circ$ and $\vartheta_2=0^\circ$ in different environments. From this, it is clear that Root-MUSIC is a high resolution DOA algorithm which can estimate two closely spaced angles of arrival as two angles and not one.

Fig. 4e and 4f depicts the accuracy of the Root-MUSIC for a signal impinging on the array specifically at 23° for varying values of array size and SNR. It can be observed that the performance of this algorithm is less dependent on the array size but largely on the operating environment but it anyhow improves with the improvement of either.

Tables I and II shows the response of the ESPRIT algorithm to varying values of SNR and array size. As in the other two algorithms, the resolution is very poor for low values of SNR and improves as the SNR values increase. Minimal variation in the accuracy of the algorithm with the array size is observed. Fig. 5 summarizes the performance of the three algorithms in terms of the Mean Square Error (MSE) and in comparison with CRLB as the values of the SNR and the array sizes are varied. Four angles of arrival $\vartheta_1 = -36^\circ$, $\vartheta_2 = -3^\circ$, $\vartheta_3 = 3^\circ$ and $\vartheta_4 = 36^\circ$ therefore become smaller with respect to the noise levels. With increase in SNR, the difference between the two sets of eigenvalues is substantial and the peaks are bigger with respect to the noise levels.

Fig. 3b depicts the response of the MUSIC algorithm to varying number of snapshots. It can be seen from the figure that for 20 snapshots the response has less pronounced spikes. The resolution is seen to improve with increase in the number of snapshots from 20 to 200,000. The number of snapshots affect the correlation between the received signals. For less snapshots, the received signals seem more correlated making it difficult to distinguish between them.

The response of MUSIC algorithm to the array size is as shown in Fig. 3c. From the figure, it can be seen that for 5 elements, the spikes are very definite and exactly correspond the the angles of arrival. As the array size increase, the resolution improves and the extraction of the angle of arrival becomes easier. An extract of the pseudospectrum for $N=5$ and $N=200$ are shown in Fig. 3d and 3e respectively.

MUSIC pseudospectrum for two closely spaced signals separated by 1° i.e. $\vartheta_1=-1^\circ$ and $\vartheta_2=0^\circ$ is captured in Fig. 3f for $N=8$ and $SNR=100dB$. From the figure, the two angles of arrival can be exactly extracted making MUSIC algorithm a high resolution DOA algorithm.

Fig. 4a shows the behaviour of root-MUSIC algorithm for varying values of SNR. From the figure, it can be seen that the accuracy is poor for 0dB SNR and improves as the SNR increases from 0dB to 100dB. The response of Root-MUSIC to variation in the array size is shown in Fig. 4b. It can be observed from the figure that the variation of the estimated angle of arrival is minimal with increase in the array size.

Fig. 4c and 4d presents two signals separated by 1° , i.e. $\vartheta_1=-0^\circ$ and $\vartheta_2 = 87^\circ$ (two closely spaced and one

near endfire). From Fig. 5a-5e, it can be observed that the MSE diminishes with increase in both SNR and array size and the performance approaches the CRLB. However, variation of MSE with the array size is flat and approaching the CRLB behaviour for ESPRIT algorithm as captured in Fig. 5f.

VII. CONCLUSION

VIII. It is clear from the foregoing discussion that the three DOA algorithms built in MATLAB and their reaction to different parameters are high resolution algorithms. This is based on how accurately the angles of arrival are calculated. The three algorithms are extremely sensitive to the signal to noise ratio (SNR), and it is discovered that as the SNR increases, the algorithms' resolution improves. The number of elements that make up the antenna array is also found to significantly boost resolution. While root-MUSIC needs comparatively more elements than MUSIC in a high SNR environment with average snapshots, MUSIC algorithms work well with an array that has few array elements in an environment with high SNR. In contrast, the ESPRIT algorithm can outperform the other two in a situation with low SNR and is less reliant on array size.

REFERENCES

- [1] "Adaptive antenna array for satellite communication systems," Proceedings of the International Multiconference of Engineers and Computer Scientists, vol. 2, March 2008, Hong Kong, by S. Kamboj and R. Dahiya.
- [2] "Direction of arrival estimation for uniform sensor arrays," International Symposium on Electronics and Telecommunication (ISETC), no. 978-1-4244-8460-7/10, 2010, A. Iozsa and A. Vesa.
- [3] International Symposium on Electronics and Telecommunication (ISETC), no. 978-1-4244-8460-7/10, 2010, A. Iozsa and A. Vesa, "The esprit algorithm. variants and precision."
- [4] "Study of signal estimation parameters via rotational invariance technique by using ants colony optimization algorithm," Eng. & Tech. Journal, vol. 29, no. 4, pp. 736–749, 2011, by A. A. Noori, S. K. Gharghan, and A. A. Wahab.
- [1] "Eigen structures based direction of arrival estimation algorithms for smart antennas systems," by M. Barkar, R. M. Vani, and P. V. Hunagund, in IJCSNS International Journal of Computer Science and Network Security, vol. 9, pp. 96–100, Nov 2009.
- [2] Benjamin Friedlander and Engin Tuncer, Direction-of-Arrival Estimation: Classical and Modern, ch. 1, pp. 10–13. Elsevier, Inc. (2009).
- [3] "Fast and accurate direction-of-arrival estimation for a single source," Y. Wu, H. Liu, and H. C. So, Progress In Electromagnetics Research C, vol. 6, pp. 13–20, 2009.
- [4] A. Vesa, "Music and the root-music algorithm for arrival estimation," 18th Telecommunication Forum TELFOR, November 2010.
- [5] "Resolution threshold analysis of music algorithm in radar range imaging," Advanced Electromagnetics Research B, vol. 31, pp. 297–321, 2011, by X. Gu and Y. H. Zhang.
- [6] "Sensitivity analysis for direction of arrival estimation using a root-music algorithm," Engineering Letters, vol. 13, pp. 353–360, 2008, by Z. Aliyazicioglu, H. K. Hwang, M. Grice, and A. Yakovlev.
- [7] "Espirit algorithm performance analysis for smart antenna system," International Journal of Communication Networks and Security, vol. 1, pp. 34–37, 2012, C. R. Dongarsane, A. N. Jadhav, and S. M. Hirikude.